Applied Mathematical Modelling 39 (2015) 2763–2776

Contents lists available at ScienceDirect

Applied Mathematical Modelling

journal homepage: www.elsevier.com/locate/apm

The oxygen diffusion problem: Analysis and numerical solution

S.L. Mitchell *, M. Vynnycky [1]

Mathematics Applications Consortium for Science and Industry (MACSI), Department of Mathematics and Statistics, University of Limerick, Limerick, Ireland

ARTICLE INFO

Article history:
Received 17 November 2013
Received in revised form 7 July 2014
Accepted 30 October 2014
Available online 25 November 2014

Keywords:
Oxygen diffusion
Moving boundary
Keller box scheme
Depletion time

ABSTRACT

A recently derived numerical algorithm for one-dimensional time-dependent Stefan problems is applied to the classical moving boundary problem that arises from the diffusion of oxygen in absorbing tissue; in tandem with the Keller box finite-difference scheme, the so-called boundary immobilization method is used. New insights are obtained into three aspects of the problem: the numerical accuracy of the scheme used; the calculation of oxygen depletion time; and the behaviour of the moving boundary as the oxygen is depleted.

1. Introduction

The one-dimensional problem of oxygen diffusion in a medium which simultaneously absorbs the oxygen, as originally posed by Crank and Gupta [1], constitutes an unusual moving boundary problem, since there is no Stefan condition which contains the velocity of the moving boundary explicitly. On the other hand, and in common with most Stefan problems, there is no analytical solution and so numerical methods are required to solve it.

There is, by now, an extensive literature on numerical solutions to the oxygen diffusion problem [2–21]. Crank and Gupta [1] considered integral methods, more commonly referred to as heat balance integral methods in relation to heat conduction problems, but these were not valid for small times and also broke down before all the oxygen had been depleted. Gupta and Banik [10] discussed a variant of Crank and Gupta's method, but their results were similar in accuracy and also had the same drawbacks. Ahmed [8,19] embedded the integral method into a numerical scheme by applying various moments of the integral formulation and created a system of linear equations. However, the resulting algorithms were complicated and their accuracy was not discussed. Mitchell [22] used a transformation to remove inconsistencies between the boundary and initial conditions and then showed that an integral method applied to the new problem yielded very accurate approximate solutions and overcame the deficiencies of previous work.

However, although it is evident that the problem has been tackled in many different ways, we focus on three aspects of the problem that have either not been resolved conclusively or not considered at all. The first concerns the formal accuracy of the numerical scheme used to solve the governing equations; this appears never to have been considered. It turns out to be of relevance in view of our recent work using the formally second-order accurate Keller box finite-difference method for moving boundary problems, where we showed that the actual accuracy of a numerical scheme decreases if inconsistencies between initial and boundary conditions are not treated correctly [23–25]; indeed, this is exactly what happens in the

* Corresponding author.
E-mail address: sarah.mitchell@ul.ie (S.L. Mitchell).
[1] Present address: Division of Casting of Metals, Department of Materials Science and Engineering, Royal Institute of Technology, Brinellvägen 23, 100 44 Stockholm, Sweden.

http://dx.doi.org/10.1016/j.apm.2014.10.068
0307-904X/

oxygen diffusion problem. The second aspect that we consider is the actual value of the time, t_e, at which the oxygen is depleted; we shall call this quantity the extinction time, in line with other physical situations where a domain that is initially of finite extent vanishes after a finite time [26–31]. Although Crank and Gupta [1] gave this some consideration, and found it to be roughly $\pi/16$, there has never been a more accurate computation to determine it. Thirdly, we consider in some detail the behaviour of the location of the moving boundary, s, as a function of time, t, as the oxygen depletes; Crank and Gupta [1] suggested that $s \sim (t_e - t)^{1/2}$, but we demonstrate that this cannot be the case and show that the problem, as classically posed, has a mathematical singularity as t_e is approached.

The layout of the paper is as follows. In Section 2, we re-cap the governing equations for the oxygen diffusion problem. In Section 3, we extract important analytical details from the problem, both in the small-time limit and as the oxygen is depleted. Section 4 explains how the resulting equations are implemented numerically using the analysis presented in Section 3; as in [23–25,32], we use the Keller box scheme in tandem with the boundary immobilization method. The results are then presented and discussed in Section 5, and conclusions are drawn in Section 6.

2. Mathematical formulation

The one-dimensional problem of oxygen diffusion in a medium which simultaneously consumes the oxygen is generally presented in two parts. First, oxygen is allowed to diffuse into the medium, which absorbs it and thereby removes it from the diffusion process. The concentration at the surface of the medium, whose location is given below by $x = 0$, is maintained constant. This first phase of the problem continues until a steady state is reached in which the oxygen does not penetrate any further into the medium. The supply of oxygen is then cut off and the surface is sealed so that no further oxygen passes in or out. The medium continues to absorb the available oxygen already there; consequently, the boundary marking the furthest depth of penetration in the steady state recedes towards the sealed surface. In this paper, we consider only the second part, for which the goal is to determine the location of the time-dependent moving boundary and the distribution of oxygen in the medium.

In nondimensional form, the problem is given by

$$\frac{\partial^2 c}{\partial x^2} = \frac{\partial c}{\partial t} + 1, \quad 0 < x < s(t), \quad 0 < t < t_e, \tag{1}$$

where c is the oxygen concentration, x is the distance from the outer surface of the medium, t is the time, $s(t)$ is the location of the oxygen front and t_e is the time taken for the oxygen to deplete. The boundary conditions are

$$\frac{\partial c}{\partial x} = 0, \quad \text{at } x = 0, \tag{2}$$

$$c = 0, \quad \text{at } x = s, \tag{3}$$

$$\frac{\partial c}{\partial x} = 0, \quad \text{at } x = s \tag{4}$$

and the initial conditions at $t = 0$ are

$$c = \frac{1}{2}(1 - x)^2, \quad s = 1. \tag{5}$$

3. Analysis

3.1. Short-time solution

As discussed by Crank and Gupta [1], the initial condition (5) shows that in the steady state a negative unit gradient of concentration exists at the surface. When the surface is sealed a zero surface gradient is instantaneously imposed in accordance with (2). There will be an interval of time, however, before the disturbance at $x = 0$ has an effect on the solution in the neighbourhood of $x = 1$. Thus, an analytical solution can be obtained for small times by assuming that the boundary $s = 1$ does not move initially.

The short-time problem is therefore

$$\frac{\partial^2 c}{\partial x^2} = \frac{\partial c}{\partial t} + 1, \quad 0 < x < 1, \tag{6}$$

$$\frac{\partial c}{\partial x} = 0, \quad \text{at } x = 0, \tag{7}$$

$$c = 0, \quad \text{at } x = 1, \tag{8}$$

$$c = \frac{1}{2}(1 - x)^2, \quad \text{at } t = 0, \tag{9}$$

which can be solved exactly using Laplace transforms or separation of variables. The former gives

$$c(x,t)=\frac{1}{2}(1-x)^2+2\sqrt{\frac{t}{\pi}}\sum_{n=0}^{\infty}(-1)^n\left[\exp\left\{-\left(\frac{2n+2-x}{2\sqrt{t}}\right)^2\right\}-\exp\left\{-\left(\frac{2n+x}{2\sqrt{t}}\right)^2\right\}\right]$$
$$-\sum_{n=0}^{\infty}(-1)^n\left[(2n+2-x)\operatorname{erfc}\left(\frac{2n+2-x}{2\sqrt{t}}\right)-(2n+x)\operatorname{erfc}\left(\frac{2n+x}{2\sqrt{t}}\right)\right], \tag{10}$$

whilst the latter leads to

$$c(x,t)=\frac{1}{2}(x^2-1)+\sum_{n=0}^{\infty}A_n\cos\left[(n+1/2)\pi x\right]\exp\left[-(n+1/2)^2\pi^2 t\right], \tag{11}$$

where

$$A_n=\frac{8}{\pi^2(4n^2+4n+1)},\quad n=0,1,2,\ldots. \tag{12}$$

The form in Eq. (10) is more convenient for determining the small time behaviour of $s(t)$. Truncating the summation at the first term gives

$$c(x,t)\sim\frac{1}{2}(1-x)^2+2\sqrt{\frac{t}{\pi}}\left[\exp\left\{-\left(\frac{2-x}{2\sqrt{t}}\right)^2\right\}-\exp\left\{-\left(\frac{x}{2\sqrt{t}}\right)^2\right\}\right]-\left[(2-x)\operatorname{erfc}\left(\frac{2-x}{2\sqrt{t}}\right)-x\operatorname{erfc}\left(\frac{x}{2\sqrt{t}}\right)\right]. \tag{13}$$

Using (13) we find that

$$c_x\sim-(1-x)+\operatorname{erfc}\left(\frac{2-x}{2\sqrt{t}}\right)+\operatorname{erfc}\left(\frac{x}{2\sqrt{t}}\right), \tag{14}$$

which can be expanded about $x=1$ to give

$$c_x\sim-(1-x)+2\operatorname{erfc}\left(\frac{1}{2\sqrt{t}}\right)+\frac{(1-x)^2}{2\sqrt{\pi}t^{3/2}}e^{-1/4t}\left[1-\frac{(1-x)^2(6t-1)}{48t^2}+\cdots\right]. \tag{15}$$

Now, for large z we have

$$\operatorname{erfc}z\sim e^{-z^2}\left[\frac{1}{\sqrt{\pi}z}-\frac{1}{2\sqrt{\pi}z^3}+\cdots\right]$$

and so

$$\operatorname{erfc}\left(\frac{1}{2\sqrt{t}}\right)\sim 2\sqrt{\frac{t}{\pi}}e^{-1/4t},$$

to leading order. If we set $1-x=f(t)$, where $f(t)\ll 1$ for $t\ll 1$, then we can use this approximation in the expansion in (15) to deduce that

$$f(t)=4\sqrt{\frac{t}{\pi}}e^{-1/4t}. \tag{16}$$

Thus

$$1-s(t)\longrightarrow 4\sqrt{\frac{t}{\pi}}e^{-1/4t},\quad \text{as } t\to 0^+. \tag{17}$$

3.2. Transformations leading to a consistent form

From the short-time solution (6)–(9), we can deduce that

$$\lim_{t\to 0}c(0,t)=\frac{1}{2}=\lim_{x\to 0}c(x,0), \tag{18}$$

showing consistency in c at $(x,t)=(0,0)$, but that the same is not true for c_x since

$$\lim_{t\to 0}c_x(0,t)=0,\quad \lim_{x\to 0}c_x(x,0)=-1; \tag{19}$$

at (1,0), on the other hand, we have that

$$\lim_{t\to 0}c(1,t)=\lim_{x\to 1}c(x,0),\quad \lim_{t\to 0}c_x(1,t)=\lim_{x\to 1}c_x(x,0),$$

so that both c and c_x are consistent there. Moreover, as explained in [23–25], consistency is important because it has an effect on the accuracy of the numerical scheme that is used; from this point of view, it is advantageous to apply a scheme to a formulation where both the dependent variable and its spatial derivative are consistent at both (0,0) and (1,0). A natural first step towards achieving this is to define a new dependent variable, u, given by

$$u(x,t) = c(x,t) - \frac{1}{2}(1-x)^2. \tag{20}$$

Substituting this into (6)–(9) gives

$$\frac{\partial^2 u}{\partial x^2} = \frac{\partial u}{\partial t}, \quad 0 < x < 1, \tag{21}$$

$$\frac{\partial u}{\partial x} = 1, \quad \text{at } x = 0, \tag{22}$$

$$u = 0, \quad \text{at } x = 1, \tag{23}$$

$$u = 0, \quad \text{at } t = 0. \tag{24}$$

Now, u_x has the same inconsistency at (0,0) as c_x, but we can now extend range of validity of (20) to the semi-infinite domain with $x \to \infty$, and replace boundary condition (23) by

$$u \to 0, \quad \text{as } x \to \infty \tag{25}$$

to give a problem having an exact analytical solution; this is

$$u(x,t) = x\,\mathrm{erfc}\left(\frac{x}{2\sqrt{t}}\right) - 2\sqrt{\frac{t}{\pi}}\exp\left(-\frac{x^2}{4t}\right). \tag{26}$$

Moreover, (26) provides precisely the extra transformation required to obtain a consistent form for u_x, and hence c_x, at (0,0); thus, defining

$$v(x,t) = c(x,t) - \frac{1}{2}(1-x)^2 - x\,\mathrm{erfc}\left(\frac{x}{2\sqrt{t}}\right) + 2\sqrt{\frac{t}{\pi}}\exp\left(-\frac{x^2}{4t}\right) \tag{27}$$

and substituting into (6)–(9), leads to the transformed problem

$$\frac{\partial^2 v}{\partial x^2} = \frac{\partial v}{\partial t}, \quad 0 < x < 1, \tag{28}$$

$$\frac{\partial v}{\partial x} = 0, \quad \text{at } x = 0, \tag{29}$$

$$v = -\mathrm{erfc}\left(\frac{1}{2\sqrt{t}}\right) + 2\sqrt{\frac{t}{\pi}}\exp\left(-\frac{1}{4t}\right), \quad \text{at } x = 1, \tag{30}$$

$$v = 0, \quad \text{at } t = 0, \tag{31}$$

which is consistent for both $v(0,0)$ and $v_x(0,0)$.

With this in mind, we now return to the full problem (1)–(5) and apply the transformation (27). This gives

$$\frac{\partial^2 v}{\partial x^2} = \frac{\partial v}{\partial t}, \quad 0 < x < s, \tag{32}$$

$$\frac{\partial v}{\partial x} = 0, \quad \text{at } x = 0, \tag{33}$$

$$v = f(s,t), \quad \text{at } x = s, \tag{34}$$

$$\frac{\partial v}{\partial x} = g(s,t), \quad \text{at } x = s, \tag{35}$$

$$v = 0, \quad s = 1, \quad \text{at } t = 0, \tag{36}$$

where

$$f(s,t) = -\frac{1}{2}(1-s)^2 - s\,\mathrm{erfc}\left(\frac{s}{2\sqrt{t}}\right) + 2\sqrt{\frac{t}{\pi}}\exp\left(-\frac{s^2}{4t}\right), \tag{37}$$

$$g(s,t) = \frac{\partial f}{\partial s} = 1 - s - \mathrm{erfc}\left(\frac{s}{2\sqrt{t}}\right). \tag{38}$$

Notice that, in spite of the transformations, the formulation is consistent for both v and v_x at (1,0), with

$$\lim_{t\to 0} v(0,t) = \lim_{x\to 0} v(x,0) = 0, \quad \lim_{t\to 0} v_x(0,t) = \lim_{x\to 0} v_x(x,0) = 0. \tag{39}$$

For the ongoing analysis and for the numerical solution, which we discuss in more detail in Section 4 below, it is convenient to use coordinates in which the boundary is immobilized. Thus, we set

$$\xi = \frac{x}{s}, \quad v(x,t) = F(\xi,t), \tag{40}$$

so that (32)–(36) become

$$\frac{\partial^2 F}{\partial \xi^2} = s^2 \frac{\partial F}{\partial t} - \xi s s_t \frac{\partial F}{\partial \xi}, \quad 0 < \xi < 1, \tag{41}$$

$$\frac{\partial F}{\partial \xi} = 0, \quad \text{at } \xi = 0, \tag{42}$$

$$F = f(s,t), \quad \text{at } \xi = 1, \tag{43}$$

$$\frac{\partial F}{\partial \xi} = s g(s,t), \quad \text{at } \xi = 1, \tag{44}$$

$$F = 0, \quad s = 1, \quad \text{at } t = 0. \tag{45}$$

3.3. Behaviour as $t \to t_e^-$

Crank and Gupta [1] noted that ds/dt tends to infinity as $t \to t_e^-$ and in particular suggested that this could be approximated by $(t_e - t)^{-1/2}$. Here, we demonstrate that this cannot be the case and we search alternative possibilities.

As we are considering the end behaviour we set $\zeta = t_e - t$ and so (41)–(44) become

$$\frac{\partial^2 F}{\partial \xi^2} = -s^2 \frac{\partial F}{\partial \zeta} + \xi s s_\zeta \frac{\partial F}{\partial \xi}, \quad 0 < \xi < 1, \quad 0 < \zeta < t_e, \tag{46}$$

$$\frac{\partial F}{\partial \xi} = 0, \quad \text{at } \xi = 0, \tag{47}$$

$$F = -\frac{1}{2}(1-s)^2 - s\,\mathrm{erfc}\left(\frac{s}{2\sqrt{t_e - \zeta}}\right) + \frac{2}{\sqrt{\pi}}\sqrt{t_e - \zeta}\exp\left(-\frac{s^2}{4(t_e - \zeta)}\right), \quad \text{at } \xi = 1, \tag{48}$$

$$\frac{\partial F}{\partial \xi} = s\left[1 - s - \mathrm{erfc}\left(\frac{s}{2\sqrt{t_e - \zeta}}\right)\right], \quad \text{at } \xi = 1. \tag{49}$$

At this stage, Eq. (46) resembles that obtained for an almost evaporated spherical droplet in [24], which led to the result that $s \sim \zeta^{1/2}$; here, however, it turns out that the boundary conditions are incompatible with this possibility, as we show in Appendix A, which in turn means that we cannot have $ds/dt \sim (t_e - t)^{-1/2}$.

To explore alternative possibilities, we first set $S = s^2$, which gives

$$\frac{\partial^2 F}{\partial \xi^2} = -S\frac{\partial F}{\partial \zeta} + \frac{1}{2}\xi S_\zeta \frac{\partial F}{\partial \xi}, \quad 0 < \xi < 1, \quad 0 < \zeta < t_e, \tag{50}$$

$$\frac{\partial F}{\partial \xi} = 0, \quad \text{at } \xi = 0, \tag{51}$$

$$F = -\frac{1}{2}\left(1 - S^{1/2}\right)^2 - S^{1/2}\,\mathrm{erfc}\left(\frac{S^{1/2}}{2\sqrt{t_e - \zeta}}\right) + \frac{2}{\sqrt{\pi}}\sqrt{t_e - \zeta}\exp\left(-\frac{S}{4(t_e - \zeta)}\right), \quad \text{at } \xi = 1, \tag{52}$$

$$\frac{\partial F}{\partial \xi} = S^{1/2}\left[1 - S^{1/2} - \mathrm{erfc}\left(\frac{S^{1/2}}{2\sqrt{t_e - \zeta}}\right)\right], \quad \text{at } \xi = 1. \tag{53}$$

We seek a separable solution of the form $F(\xi,\zeta) = F_0 + S(\zeta)\phi(\xi)$, where F_0 is an unknown constant that is to be determined; in fact, it is quickly evident from Eqs. (50)–(53) at $\mathcal{O}(1)$ that

$$F_0 = 2\left(\frac{t_e}{\pi}\right)^{1/2} - \frac{1}{2}. \tag{54}$$

The left-hand side of (50) is $O(S)$, whereas the two terms on the right-hand side are nominally $\mathcal{O}(SS_\zeta)$, and hence much greater than the term on the left-hand side. We will suppose that the two terms on the right-hand side balance each other; this is the only other option available, since the approach in Appendix A already allows for the possibility that the term arising on the left-hand side balances those on the right. Thence, we obtain

$$\frac{1}{2}\xi\phi' - \phi = 0, \tag{55}$$

subject to

$$\phi'(0) = 0, \tag{56}$$

$$\phi(1) = \frac{1}{2}\left(\frac{1}{\sqrt{\pi t_e}} - 1\right), \tag{57}$$

$$\phi'(1) = \frac{1}{\sqrt{\pi t_e}} - 1. \tag{58}$$

Surprisingly, even though we require a first-order ordinary differential equation to satisfy three boundary conditions, the solution

$$\phi = \frac{1}{2}\left(\frac{1}{\sqrt{\pi t_e}} - 1\right)\xi^2 \tag{59}$$

does just this. However, S is still undetermined, although it must tend to zero more slowly than ζ in order to ensure that the term in SS_ζ in Eq. (50) dominates the term in S. Returning to s and t, this suggests that s tends to zero more slowly than $(t_e - t)^{1/2}$, which helps in part to explain why the approach given in Appendix A fails.

It is also worth determining what happens at the order after $O(S)$. Eq. (50) suggests that this should be at $O(\zeta)$, so we set

$$F(\xi, \zeta) = F_0 + S(\zeta)\phi(\xi) + \zeta\varphi(\xi),$$

which leads to

$$\phi'' = -\varphi + \frac{1}{2}v\xi\varphi', \quad 0 < \xi < 1, \tag{60}$$

subject to

$$\varphi' = 0, \quad \text{at } \xi = 0 \tag{61}$$

$$\varphi = -\frac{1}{\sqrt{\pi t_e}}, \quad \text{at } \xi = 1 \tag{62}$$

$$\varphi' = 0, \quad \text{at } \xi = 1, \tag{63}$$

where $v = \lim_{\zeta\to 0}\zeta S_\zeta/S$. So, (60) gives

$$\frac{1}{2}v\xi\varphi' - \varphi = \frac{1}{\sqrt{\pi t_e}} - 1,$$

whence

$$\varphi = C\xi^{2/v} + 1 - \frac{1}{\sqrt{\pi t_e}},$$

where C is a constant to be determined from the boundary conditions. However, whereas (61) can be satisfied for any value of C, (63) requires that $C = 0$, which then implies that (62) cannot be satisfied; consequently, this approach also breaks down.

In summary, although the analysis has been unable to determine the behaviour of S as $\zeta \to 0$, it has indicated that S tends to zero more slowly than ζ. Furthermore, because $\chi = 1$, it is not possible that $S \sim \zeta^\alpha$, where $0 < \alpha < 1$. This perhaps suggests logarithmic behaviour, e.g. $S \sim \zeta(-\ln\zeta)^\beta$, where $\beta > 0$, although our analysis should have picked this out, had this really been the case. Alternatively, this may simply be suggesting that either there is no similarity-like asymptotic solution structure as $t \to t_e^-$, or that the system of equations – in particular, this combination of boundary conditions – leads to a problem that is ill-posed. The onus is then on the numerical work to explain what happens.

4. Numerical method

4.1. Discussion

So far, the basic governing equations have been rewritten in several different forms, each of which has been used to obtain analytical details regarding the solution. However, it is not obvious which one of these is most appropriate for numerical implementation, in view of the demands we have on the quality of the solution. These are:

- that the solution is second-order accurate in both time and space for the concentration, the concentration flux and the location of the moving boundary, in line with our earlier work;
- that the value of t_e is also found with second-order accuracy;
- that the analytical behaviour of s is resolved as $t \to t_e$.

Here, we will once again focus on developing a scheme based on the Keller box method, in tandem with boundary immobilization. We have previously shown that although the Keller box method is formally second-order accurate, accuracy is lost

if there is an inconsistency between the initial conditions and the boundary conditions [23–25]. As discussed in Section 3.2, we mean that there is an inconsistency in a function ψ, where $\psi = c$ or c_x, if

$$\lim_{x\to 0}\psi(x,0) \neq \lim_{t\to 0}\psi(0,t) \quad \text{or} \quad \lim_{x\to 1}\psi(x,0) \neq \lim_{t\to 0}\psi(1,t).$$

This suggests immediately that discretising Eqs. (1)–(4) as they stand will not give a scheme that is second-order accurate; more hopeful would be to discretise (32)–(36), or (41)–(45) after the transformation to immobilize the boundary. However, we have also previously found that even if there is consistency for a function and its first spatial derivative, this will still not necessarily give a scheme that has second-order accuracy for the first spatial derivative [25]. However, and perhaps rather fortuitously in the present case, the transformation used to obtain (32)–(36) from (1)–(4) ensures not only that v and v_x were consistent at (0,0) and (1,0), but that v_{xx} is consistent at these locations also. To see this, note first that v_{xx} will be consistent near (0,0) because we have already subtracted off the solution to the governing equation which satisfies both the initial condition at $t = 0$ and the boundary condition at $x = 0$; near (1,0), on the other hand, we note that

$$\lim_{x\to 1} v_{xx}(x,0) = 0, \quad \lim_{t\to 0} v_{xx}(1,t) = 0$$

with the second, less obvious, equality coming from using Eqs. (17), (32), (34) and (37). Consequently, these observations suggest that the resulting numerical solution may indeed have second-order accuracy for v_{xx} also.

Far trickier is how to find t_e, since even by discretising and solving (41)–(45) it is not clear how to predict this value numerically. The issue of Stefan problems having a starting or a stopping time, meaning that the moving boundary appears or disappears in the course of a computation, but is not present for all of it, has been touched on by us previously in the contexts of ablation [23], droplet evaporation [24] and the continuous casting of metals [27,28,33,34], although without an adequate resolution in those cases. Here, however, we adopt the approach taken in [35] by setting $t = t_e\tau$, so that all integrations are performed for $0 \leqslant \tau \leqslant 1$, but with t_e to be determined along with the location of the moving boundary; we give more details of the implementation later. Furthermore, since the analysis in Section 3 has already hinted that ds/dt may have a singularity as $t \to t_e$, the use of the transformation $S = s^2$ appears to be advantageous. Implementing these considerations, we have

$$t_e\frac{\partial^2 F}{\partial \xi^2} = S\frac{\partial F}{\partial \tau} - \frac{1}{2}\xi S_\tau\frac{\partial F}{\partial \xi}, \quad 0 < \xi < 1, \quad 0 < \tau < 1, \tag{64}$$

$$\frac{\partial F}{\partial \xi} = 0, \quad \text{at } \xi = 0, \tag{65}$$

$$F = -\frac{1}{2}\left(1 - S^{1/2}\right)^2 - S^{1/2}\,\mathrm{erfc}\left(\frac{S^{1/2}}{2\sqrt{t_e\tau}}\right) + 2\sqrt{\frac{t_e\tau}{\pi}}\exp\left(-\frac{S}{4t_e\tau}\right), \quad \text{at } \xi = 1, \tag{66}$$

$$\frac{\partial F}{\partial \xi} = S^{1/2}\left[1 - S^{1/2} - \mathrm{erfc}\left(\frac{S^{1/2}}{2\sqrt{t_e\tau}}\right)\right], \quad \text{at } \xi = 1, \tag{67}$$

$$F = 0, \quad S = 1, \quad \text{at } \tau = 0. \tag{68}$$

In addition, and related to the resolution of behaviour of the solution as $t \to t_e$, it is beneficial to introduce an appropriate stretching in the variable τ as $\tau \to 1$; although there is no unique way to do this, we will chose

$$1 - \tau = \exp(-\hat{\tau}), \quad \text{where } 0 \leqslant \hat{\tau} < \infty. \tag{69}$$

In the interests of brevity, we have not included here the transformed version of Eqs. (64)–(68). In practice, it is of course necessary to terminate the computations at some finite value of $\hat{\tau}$, which we denote as $\hat{\tau}_\infty$; we have taken $\hat{\tau}_\infty$ so that $1 - \tau = \mathcal{O}(10^{-9})$, implying that $\hat{\tau}_\infty = 20$.

Lastly, we note one of the *disadvantages* of this new formulation. The parameter t_e now appears explicitly in the governing equations, yet its value is not known *a priori*; consequently, we cannot find the solution at any value of x and t before we find t_e. On the other hand, the original formulation, Eqs. (41)–(45), *does* enable us to find the solution at any value of x and t before we find t_e, but does not give us a strategy for finding t_e. Therefore, in what follows, we will implement discretization schemes for both formulations.

4.2. Discretization schemes

To apply the Keller box scheme [23,24,32] to Eqs. (41)–(45), we re-write (41) as a first-order system by setting $F_\xi = G$. For a general dependent variable Φ and general independent time- and space-like variables, X and Y respectively, we define the following finite difference operators:

$$\mu_X\Phi^{n+\frac{1}{2}}_{i+\frac{1}{2}} = \frac{\Phi^{n+1}_{i+\frac{1}{2}} + \Phi^{n}_{i+\frac{1}{2}}}{2}, \quad \delta_X\Phi^{n+\frac{1}{2}}_{i+\frac{1}{2}} = \frac{\Phi^{n+1}_{i+\frac{1}{2}} - \Phi^{n}_{i+\frac{1}{2}}}{\Delta X}, \tag{70}$$

$$\mu_Y\Phi^{n+\frac{1}{2}}_{i+\frac{1}{2}} = \frac{\Phi^{n+\frac{1}{2}}_{i+1} + \Phi^{n+\frac{1}{2}}_{i}}{2}, \quad \delta_Y\Phi^{n+\frac{1}{2}}_{i+\frac{1}{2}} = \frac{\Phi^{n+\frac{1}{2}}_{i+1} - \Phi^{n+\frac{1}{2}}_{i}}{\Delta Y}. \tag{71}$$

With $X = t,\ Y = \xi$, the box scheme applied, for example, to (41) therefore gives, for $n = 0, 1, 2, \ldots$,

$$\mu_t \delta_\xi F^{n+\frac{1}{2}}_{i+\frac{1}{2}} = \mu_t \mu_\xi G^{n+\frac{1}{2}}_{i+\frac{1}{2}}, \tag{72}$$

$$\mu_t \delta_\xi G^{n+\frac{1}{2}}_{i+\frac{1}{2}} = \left(\mu_t s^{n+\frac{1}{2}}\right)^2 \left(\mu_\xi \delta_t F^{n+\frac{1}{2}}_{i+\frac{1}{2}}\right) - \left(\mu_\xi \xi_{i+\frac{1}{2}}\right)\left(\mu_t s^{n+\frac{1}{2}}\right)\left(\delta_t s^{n+\frac{1}{2}}\right)\left(\mu_\xi G^{n+\frac{1}{2}}_{i+\frac{1}{2}}\right), \tag{73}$$

which holds for $i = 1, \ldots, I-1$. Note that $\xi_i = i\Delta\xi$, for $i = 0, 1, \ldots, I$, with $\Delta\xi = 1/I$. Boundary condition (42) is simply $G^n_0 = 0$, for $n = 0, 1, 2, \ldots$, and conditions (43) and (44) are

$$\frac{1}{2}\left(F^{n+1}_I + F^n_I\right) = \frac{1}{2}(f^{n+1} + f^n), \tag{74}$$

$$\frac{1}{2}\left(G^{n+1}_I + G^n_I\right) = \frac{1}{2}(g^{n+1} + g^n) \tag{75}$$

for $n = 0, 1, 2, \ldots$. Finally, the initial conditions in (45) become $F^0_i = G^0_i = 0$, for $i = 1, \ldots, I$, and $s^0 = 1$.

It should be noted that Eqs. (73)–(75) involve s^{n+1} and so it is necessary to solve a nonlinear equation at each timestep. For more standard Stefan-like problems [23,24,32], where there is an explicit expression for the speed of the moving boundary s_t (say), this is achieved by iterating on s. The value at level n is used as a starting guess, and then updated by solving the discretised Stefan condition until some desired tolerance is reached. However, since there is no Stefan condition for the oxygen diffusion problem, we cannot follow the same approach here. Instead, at each timestep we use a nonlinear solver (such as `fzero` in Matlab) to determine s^{n+1}, with the value at the n^{th} level used as a starting guess. The nonlinear equation can be either of the boundary conditions (74) or (75).

For the formulation given by Eqs. (64)–(68), and as already mentioned, the value of t_e is unknown *a priori* and must be determined, along with $F,\ G = (F_\xi)$ and S, as part of the solution process. The time domain is now fixed and so we can choose N points whereby $\hat{\tau}^n = n\Delta\hat{\tau}$, for $n = 0, 1, \ldots, N$, and with $\Delta\hat{\tau} = 1/N$. The simplest way to do this is to use a nonlinear solver to determine S^n, for $n = 1, 2, \ldots, N$, along with t_e, leading to $N+1$ unknowns. One of the boundary conditions (66), (67) can be used to give N nonlinear equations and then the final equation is simply $S^N = 0$. In practice, we make an initial guess for t_e and solve for F and S up to $\hat{\tau} = \hat{\tau}_\infty$; in general, we will obtain $S^N \neq 0$, but the discrepancy can be used as a basis for making a new guess for t_e, and re-solving. This procedure is then repeated until the desired tolerance is reached. Denoting by $S^N_{(m)}$ the value of S^N obtained on the mth iteration, the convergence criterion used is

$$\left|Z^N_{(m)}\right| < \epsilon.$$

The value of ϵ used turns out to be of particular importance for the numerical solution in the limit as $t \to t_e^-$; we examine this in more detail in Section 5.3.

4.3. Order of accuracy

We will also wish to determine the order of accuracy of the scheme and of the solution. To this end, we consider a sequence $\Delta\xi_k$ where

$$\Delta\xi_k = 2^{-k}\Delta\xi_0, \quad k = 1, 2, \ldots$$

and we denote the space coordinates of meshes associated with this sequence by

$$\xi_{i,k} = i\Delta\xi_k, \quad i = 0, 1, \ldots, I_k, \quad k = 0, 1, 2, \ldots,$$

where

$$I_k = 2^k I_0, \quad k = 1, 2, \ldots.$$

As discussed in [36], for a general numerical solution $F^n_{2^k i}$ and corresponding exact solution $f(\xi_{i,k}, t^n)$ at the nth time step, t^n, the error and corresponding order of convergence, $E^n_{F,k}$ and $p_{F,k}$ respectively, are given by

$$E^n_{F,k} = \left(\Delta\xi_k \sum_{i=0}^{I_0}\left(f(\eta_{i,0}, \tau^n) - F^n_{2^k i}\right)^2\right)^{1/2}, \quad p_{F,k} = \frac{\ln(E^n_{F,k}/E^n_{F,k+1})}{\ln 2}, \tag{76}$$

for $k = 0, 1, 2, \ldots$; furthermore, the accuracy of the solution with respect to $F,\ p_F$, is then

$$p_F = \lim_{k\to\infty} p_{F,k}. \tag{77}$$

Regarding the accuracy of the scheme with respect to $F,\ \bar{p}_F$, we first define

$$\bar{E}^n_{F,k} = \left(\sum_{i=0}^{I_0}\left(F^n_{2^k i} - F^n_{2^{k-1} i}\right)^2\right)^{1/2}, \quad \bar{p}_{F,k} = \ln(\bar{E}^n_{F,k}/\bar{E}^n_{F,k+1})/\ln 2 \tag{78}$$

for $k = 1, 2, \ldots$; then,

$$\bar{p}_F = \lim_{k\to\infty} \bar{p}_{F,k}. \tag{79}$$

In cases where an exact solution was known and there were no discontinuities in the boundary conditions after reformulation, Mitchell and Vynnycky [32] showed that $p_F = \bar{p}_F$. Furthermore, Mitchell et al. [24] demonstrated that it was also possible to apply this idea to the spatial derivative of F, i.e., $G = F_\xi$. Thus, we set, for $k = 0, 1, 2, \ldots$,

$$E^n_{G,k} = \left(\Delta\check{\xi}_k \sum_{i=0}^{I_0} \left(g(\eta_{i,0}, \tau^n) - G^n_{2^k i}\right)^2\right)^{1/2}, \quad p_{G,k} = \frac{\ln\left(E^n_{G,k}/E^n_{G,k+1}\right)}{\ln 2}, \tag{80}$$

where $g = f_\xi$, and

$$\bar{E}^n_{G,k} = \left(\sum_{i=0}^{I_0} \left(G^n_{2^k i} - G^n_{2^{k-1} i}\right)^2\right)^{1/2}, \quad \bar{p}_{G,k} = \ln\left(\bar{E}^n_{G,k}/\bar{E}^n_{G,k+1}\right)/\ln 2 \tag{81}$$

for $k = 1, 2, \ldots$. In the same way, we can also consider the accuracy of s, by defining p_s and $\bar{p}_s$ through

$$E^n_{s,k} = \left|s^n_k - s(t^n)\right|, \quad k = 0, 1, 2, \ldots, \quad p_{s,k} = \frac{\ln\left(E^n_{s,k}/E^n_{s,k+1}\right)}{\ln 2}, \tag{82}$$

$$\bar{E}^n_{s,k} = \left|s^n_k - s^n_{k-1}\right|, \quad k = 1, 2, \ldots, \quad \bar{p}_{s,k} = \frac{\ln\left(\bar{E}^n_{s,k}/\bar{E}^n_{s,k+1}\right)}{\ln 2}. \tag{83}$$

In addition, we will also need to consider the accuracy of t_e; for this, we define p_{t_e} and $\bar{p}_{t_e}$ through

$$E_{t_e,k} = \left|t_{e,k} - t_e\right|, \quad k = 0, 1, 2, \ldots, \quad p_{t_e,k} = \frac{\ln\left(E_{t_e,k}/E_{t_e,k+1}\right)}{\ln 2}, \tag{84}$$

$$\bar{E}_{t_e,k} = \left|t_{e,k} - t_{e,k-1}\right|, \quad k = 1, 2, \ldots, \quad \bar{p}_{t_e,k} = \frac{\ln\left(\bar{E}_{t_e,k}/\bar{E}_{t_e,k+1}\right)}{\ln 2}. \tag{85}$$

5. Results

In summary, we present results from four different formulations:

(I) Eqs. (6)–(9);
(II) Eqs. (28)–(31);
(III) Eqs. (41)–(45);
(IV) Eqs. (64)–(68) with transformation (69).

In fact, results from all of these prove necessary to provide a complete picture of the solution to the problem.

5.1. Short-time solution

It is instructive to first consider results for the box scheme applied to the short-time problem. Although there is no moving boundary position s to evaluate, the problem does have an exact solution and so we can determine both p and $\bar{p}$ for the concentration and its first spatial derivative. Convergence results for the box scheme applied to Eqs. (28)–(31) are shown in Table 1. In Table 2 we give the results for the box scheme applied to (6)–(9), to highlight the fact that the transformation in (27) is indeed necessary to obtain second order convergence for both the concentration and its derivative.

5.2. Results for the full problem

Table 3 shows convergence results for the box scheme applied to formulation III, whereas Table 4 shows the corresponding results for formulation IV. In addition, Table 5 shows the results for t_e and $\bar{p}_{t_e}$ for formulation IV. From these tables, it is clear that both formulations give second-order accurate solutions, although formulation IV has the added advantage that it can compute t_e also. Fig. 1 compares the profiles for s obtained via the two formulations.

5.3. $t \to t_e$

In the remaining figures, we examine the performance of formulation IV in the limit as $t \to t_e$; unless otherwise stated, we take $\epsilon = 10^{-8}$. Setting $\zeta = 1 - \tau$, Fig. 2 shows S as a function of ζ for $k = 2, 3, 4$; comparison is made with the profile $S = \zeta$. From this plot, it appears that the behaviour of the solution for S is given by

Table 1
Comparison of the order of accuracy of the numerical solution of II, for v and $w(=v_x)$ at fixed $t=0.1$ and $\nu(=\Delta t/\Delta x)=0.1$.

Δx (k)	p_v	$\bar{p}_v$	p_w	$\bar{p}_w$
1/20 $(k=1)$	2.02657		2.01773	
1/40 $(k=2)$	2.00711	2.03655	2.00480	2.02596
1/80 $(k=3)$	2.00181	2.00911	2.00130	2.00656
1/160 $(k=4)$	2.00046	2.00227	2.00037	2.00164
1/320 $(k=5)$	2.00011	2.00057	2.00012	2.00041
1/640 $(k=6)$	2.00003	2.00014	2.00004	2.00010

Table 2
Comparison of the order of accuracy of the numerical solution of I, for c and $d(=c_x)$ at fixed $t=0.1$ and $\nu(=\Delta t/\Delta x)=0.1$.

Δx (k)	p_c	$\bar{p}_c$	p_d	$\bar{p}_d$
1/20 $(k=1)$	1.09607		1.23590	
1/40 $(k=2)$	1.05040	1.08858	1.13169	1.35244
1/80 $(k=3)$	1.02587	1.04090	1.07045	1.29692
1/160 $(k=4)$	1.01312	1.02153	1.03657	1.28082
1/320 $(k=5)$	1.00660	1.00960	1.01865	1.02363
1/640 $(k=6)$	1.00331	1.00477	1.00942	1.01244

Table 3
Comparison of the order of accuracy of the numerical solution for formulation III, for F, $G(=F_\xi)$ and s at fixed $t=0.15$ and $\nu(=\Delta t/\Delta\xi)=0.15$.

$\Delta\xi$ (k)	$\bar{p}_F$	$\bar{p}_G$	$\bar{p}_s$
1/40 $(k=2)$	2.03233	2.02971	1.91453
1/80 $(k=3)$	2.00757	2.00603	1.99066
1/160 $(k=4)$	2.00190	2.00151	1.99751
1/320 $(k=5)$	2.00047	2.00038	1.99937
1/640 $(k=6)$	2.00012	2.00009	1.99984

Table 4
Comparison of the order of accuracy of the numerical solution for formulation IV, for F, $G\,(=F_\xi)$ at fixed $\hat{\tau}=2.5$, and S, t_e, with $\nu(=\Delta t/\Delta\xi)=1$ and $\hat{\tau}_\infty=25$.

$\Delta\xi$ (k)	$\bar{p}_F$	$\bar{p}_G$	$\bar{p}_S$
1/80 $(k=2)$	2.00445	2.00407	2.00474
1/160 $(k=3)$	2.00114	2.00117	2.00096
1/320 $(k=4)$	2.00028	2.00033	1.99998

Table 5
t_e and $\bar{p}_{t_e}$ for $k=0,1,\ldots,4$, as predicted with formulation IV. Note that $\pi/16\approx 0.196349$.

k	0	1	2	3	4
t_e	0.197425	0.197432	0.197434	0.197435	0.197435
$\bar{p}_{t_e}$	–	–	2.00429	2.00105	1.99970

$$S=\lambda\zeta+O(\zeta^2); \tag{86}$$

however, the analysis in Appendix A indicates that this cannot be the case, since the constant of proportionality in (86), λ, cannot be found. A comparison with the result in [37], for another problem having an extinction time in which such a constant could be found, is therefore instructive. It seems plausible that any numerical discretisation and solution of the problem – not just the one presented here – leads to a perturbed problem, as discussed in Appendix A. This results in a problem for which λ can be found and is given, for example, by Eq. (A17).

A further indication that the current problem is different from that in [37] is given in Figs. 3 and 4, again for formulation IV, which show $\zeta S_\zeta/S$ as a function of ζ. For the behaviour given by Eq. (86), we would have

$$\lim_{\zeta\to 0}\zeta S_\zeta/S=1. \tag{87}$$

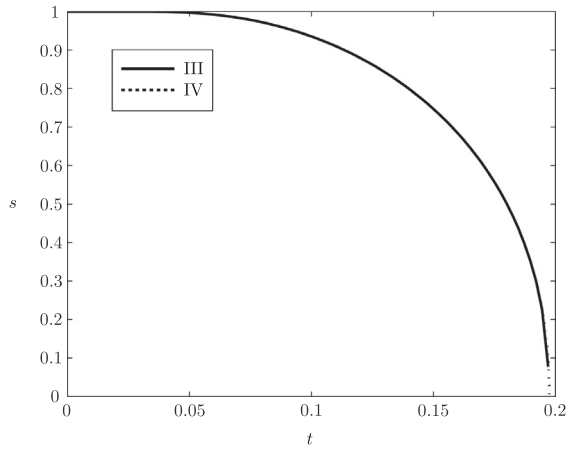

Fig. 1. s vs t for formulations III and IV.

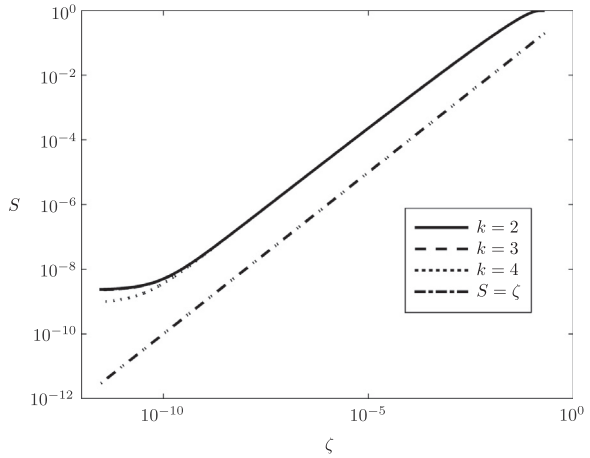

Fig. 2. S vs ζ for formulation IV ($k = 2, 3, 4$) and the line $S = \zeta$.

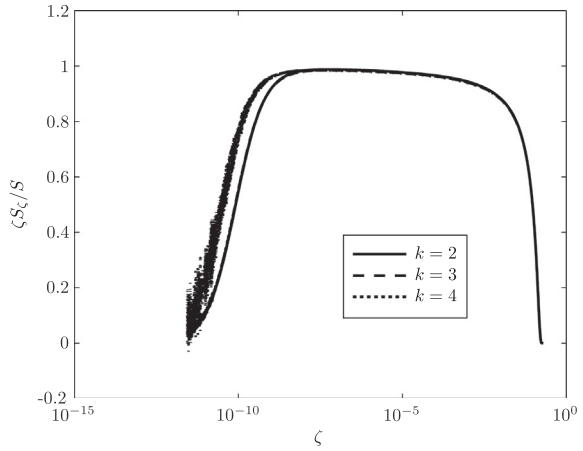

Fig. 3. $\zeta S_\zeta / S$ vs ζ for formulation IV ($k = 2, 3, 4$).

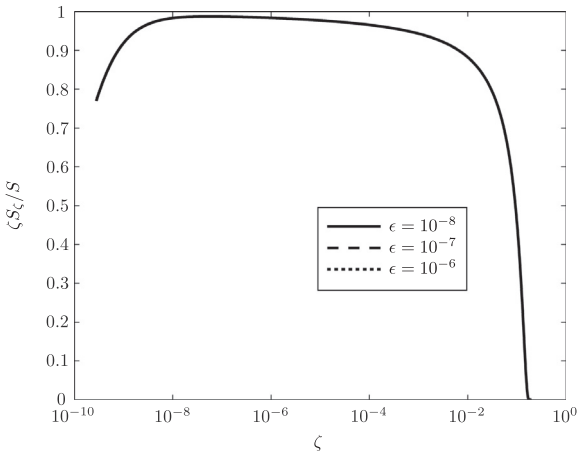

Fig. 4. $\zeta S_\zeta/S$ vs ζ for formulation IV with $k = 4$ ($\epsilon = 10^{-8}, 10^{-7}, 10^{-6}$).

In fact, Fig. 3, which shows the dependence on $k = 2, 3, 4$, indicates a behaviour that is similar to that in [37], in that there is an undesired dip for $\zeta \leqslant 10^{-8}$, which was investigated in detail [37]; however, it also evident that although the numerical solution hints at the behaviour of (87) for $10^{-8} \leqslant \zeta \ll 1$, it is not actually realised. The decisive difference between this problem and that in [37] comes in Fig. 4, which shows $\zeta S_\zeta/S$ as a function of ζ for $k = 4$, but for three different values of ϵ, and again for formulation IV. From this figure, it is evident that the value of ϵ chosen has no effect at all on the value of ζ at which the dip begins to appear in $\zeta S_\zeta/S$; in [37], on the other hand, it did, which suggested that, by decreasing ϵ, it would be possible to shift the onset of numerical oscillations to smaller values of ζ, albeit at greater computational expense. This seems to confirm that the oxygen diffusion, as classically posed, has a mathematical singularity at the extinction time.

6. Conclusions

In this paper, we have developed a numerical algorithm, based around the Keller box finite-difference scheme and the boundary immobilization method, for solving the classical moving boundary problem that arises from the diffusion of oxygen in absorbing tissue. The algorithm was shown to be second-order accurate in both time and space variables. Numerical work was complemented with analysis, which showed that the problem, as posed originally by Crank and Gupta [1], has a singularity as the oxygen depletion (extinction) time, t_e, is approached. However, any numerical attempt to solve the problem will always lead to a perturbed problem, as a result of discretization errors. This will give the impression that depletion occurs as $(t_e - t)^{1/2}$, which was the behaviour originally suggested in [1], although we have now shown that this in fact cannot be the case.

Acknowledgements

The authors acknowledge the support of the Mathematics Applications Consortium for Science and Industry (MACSI, www.macsi.ul.ie) funded by the Science Foundation Ireland Grant SFI/12/IA/1683.

Appendix A

Assume a similarity-type solution near $\zeta = 0$ of the form

$$s(\zeta) \sim \lambda\zeta^a, \quad F(\xi, \zeta) = F_0 + \zeta^b\phi(\xi), \tag{A1}$$

where a, b and λ are constants to be determined. Then (46)–(49) become

$$\phi'' = -\lambda^2 b\zeta^{2a-1}\phi + \lambda^2 a\zeta^{2a-1}\xi\phi', \quad 0 < \xi < 1, \tag{A2}$$

where the primes denote differentiation with respect to ξ, subject to

$$\phi'(0) = 0, \tag{A3}$$

$$F_0 + \zeta^b\phi(1) = -\frac{1}{2}(1 - \lambda\zeta^a)^2 - \lambda\zeta^a \operatorname{erfc}\left(\frac{\lambda\zeta^a}{2\sqrt{t_e - \zeta}}\right) + \frac{2}{\sqrt{\pi}}\sqrt{t_e - \zeta}\exp\left(-\frac{\lambda^2\zeta^{2a}}{4(t_e - \zeta)}\right), \tag{A4}$$

$$\zeta^b\phi'(1) = \lambda\zeta^a\left[1 - \lambda\zeta^a - \mathrm{erfc}\left(\frac{\lambda\zeta^a}{2\sqrt{t_e - \zeta}}\right)\right]. \tag{A5}$$

Eq. (A2) shows that $a = 1/2$ and hence $b = 2a$ from (A5). Then, (A4) and (A5) can be expanded as

$$F_0 + \zeta\phi(1) = -\frac{1}{2}\left[1 - 2\lambda\zeta^{1/2} + \lambda^2\zeta\right] - \lambda\zeta^{1/2}\left[1 - \frac{\lambda\zeta^{1/2}}{\sqrt{\pi t_e}} + \mathcal{O}(\zeta^{3/2})\right] + \frac{2}{\sqrt{\pi}}\left[\sqrt{t_e} - \frac{(\lambda^2+2)}{4\sqrt{t_e}}\zeta + \mathcal{O}(\zeta^2)\right], \tag{A6}$$

$$\zeta^{1/2}\phi'(1) = \left[-\lambda\zeta^{1/2} + \frac{\lambda\zeta^{1/2}}{\sqrt{\pi t_e}} + \mathcal{O}(\zeta^{3/2})\right], \tag{A7}$$

respectively. From (A6), the leading terms are

$$F_0 = 2\sqrt{\frac{t_e}{\pi}} - \frac{1}{2} \tag{A8}$$

and we are left solving

$$\phi'' = -\lambda^2\phi + \frac{\lambda^2}{2}\xi\phi', \quad 0 < \xi < 1, \tag{A9}$$

subject to

$$\phi'(0) = 0, \tag{A10}$$

$$\phi(1) = \frac{1}{2}\lambda^2\left(\frac{1}{\sqrt{\pi t_e}} - 1\right) - \frac{1}{\sqrt{\pi t_e}}, \tag{A11}$$

$$\phi'(1) = \lambda^2\left(\frac{1}{\sqrt{\pi t_e}} - 1\right); \tag{A12}$$

note that Eqs. (A6) and (A7) are at $\mathcal{O}(\zeta)$ since the $\mathcal{O}(\zeta^{1/2})$ terms cancel. The general solution of (A9) is

$$\phi(\xi) = C_1(-2 + \lambda^2\xi^2) + C_2\left[\sqrt{\pi}(-2 + \lambda^2\xi^2)\mathrm{erfi}\left(\frac{\lambda\xi}{2}\right) - 2\lambda\xi e^{\lambda^2\xi^2/4}\right], \tag{A13}$$

where C_1 and C_2 are constants to be determined, and erfi denotes the imaginary error function and is given by

$$\mathrm{erfi}(x) = \frac{2}{\sqrt{\pi}}\int_0^x \mathrm{e}^{z^2}\,dz.$$

Since $\mathrm{erfi}(0) = 0$, boundary condition (A10) gives that $C_2 = 0$, whereas (A11) and (A12) give

$$C_1(\lambda^2 - 2) + \frac{1}{\sqrt{\pi t_e}} = \frac{\lambda^2}{2}\left(\frac{1}{\sqrt{\pi t_e}} - 1\right), \tag{A14}$$

$$2C_1 = \frac{1}{\sqrt{\pi t_e}} - 1, \tag{A15}$$

respectively. However, substituting the expression for C_1 from (A15) into (A14) leads to an inconsistency, since the terms in λ^2 cancel, leaving λ undetermined and with the left-hand side of (A14) incompatible with the right-hand side: they give one and zero, respectively.

To understand what has happened, suppose we consider the perturbed problem where we replace (A10) by

$$\phi'(0) = \varepsilon \tag{A16}$$

with $\epsilon \neq 0$; note that we could also have perturbed either (A11) or (A12), but perturbing (A10) is more instructive and algebraically simpler. With, from Eq. (A13),

$$\phi'(\xi) = 2C_1\lambda^2\xi + 2\lambda C_2\left[\sqrt{\pi}\lambda\xi\mathrm{erfi}\left(\frac{\lambda\xi}{2}\right) - 2e^{\lambda^2\xi^2/4}\right],$$

Eqs. (A10)–(A12) give, respectively,

$$C_2 = -\frac{\varepsilon}{4\lambda},$$

$$C_1(\lambda^2 - 2) + C_2\left[\sqrt{\pi}(\lambda^2 - 2)\mathrm{erfi}\left(\frac{\lambda}{2}\right) - 2\lambda e^{\lambda^2/4}\right] = \frac{1}{2}\lambda^2\left(\frac{1}{\sqrt{\pi t_e}} - 1\right) - \frac{1}{\sqrt{\pi t_e}},$$

$$C_1\lambda + C_2\left[\sqrt{\pi}\lambda\mathrm{erfi}\left(\frac{\lambda}{2}\right) - 2e^{\lambda^2/4}\right] = \frac{1}{2}\lambda\left(\frac{1}{\sqrt{\pi t_e}} - 1\right).$$

We can then eliminate C_1 and C_2 to obtain

$$\frac{4\lambda}{\varepsilon} = \sqrt{\pi}(\lambda^2 - 2)(1 - \lambda)\mathrm{erfi}\left(\frac{\lambda}{2}\right) + 2(\lambda - 2)(\lambda + 1)e^{\lambda^2/4}; \tag{A17}$$

this explains why it was easiest to perturb Eq. (A10), since t_e has dropped out of this equation completely. Now, if $\varepsilon \ll 1$, we see that, at leading order in ε, Eq. (A17) gives $\lambda \approx -\varepsilon$, which makes physical sense only if $\varepsilon < 0$, since we must have $\lambda > 0$. Hence, if $\varepsilon = 0$, then $\lambda = 0$, rendering (A1) invalid.

References

[1] J. Crank, R.S. Gupta, A moving boundary problem arising from the diffusion of oxygen in absorbing tissue, J. Inst. Maths Applics 10 (1972) 19–33.
[2] J. Crank, R.S. Gupta, A method for solving moving boundary problems in heat flow using cubic splines or polynomials, J. Inst. Maths Applics 10 (1972) 296–304.
[3] E. Hansen, P. Hougaard, On a moving boundary problem from biomechanics, J. Inst. Maths Applics 13 (1974) 385–398.
[4] V. Gülkaç, Comparative study between two numerical methods for oxygen diffusion problem, Commun. Numer. Methods Eng. 25 (2009) 855–863.
[5] R.S. Gupta, A. Kumar, Complete numerical solution of the oxygen diffusion problem involving a moving boundary, Comput. Methods Appl. Mech. Eng. 29 (1981) 233–239.
[6] R.S. Gupta, A. Kumar, Variable time step method with coordinate transformation, Comput. Methods Appl. Mech. Eng. 44 (1984) 91–103.
[7] A.I. Liapis, G.G. Lipscom, O.K. Crosser, A model of oxygen diffusion in absorbing tissue, Math. Model. 3 (1982) 83–92.
[8] S.G. Ahmed, An approximate method for oxygen diffusion in a sphere with simultaneous absorption, Int. J. Numer. Methods Heat Fluid Flow 9 (1999) 631–642.
[9] S. Çatal, Numerical approximation for the oxygen diffusion problem, Appl. Math. Comput. 145 (2003) 361–369.
[10] R.S. Gupta, N.C. Banik, Approximate method for the oxygen diffusion problem, Int. J. Heat Mass Transfer 32 (1989) 781–783.
[11] A.E. Berger, M. Ciment, J.C.W. Rogers, Numerical solution of a diffusion consumption problem with a moving free boundary, SIAM J. Numer. Anal. 12 (1975) 646–672.
[12] D.H. Ferris, S. Hill, On the numerical solution of a one-dimensional diffusion problem with a moving boundary, Tech. Rep., NPL Report NAC 45, 1974.
[13] H.O. Dahmardah, D.F. Mayers, Fourier series solution of the Crank–Gupta equation, SIAM J. Numer. Anal. 12 (1975) 646–672.
[14] J.V. Miller, K.W. Morton, M.J. Baines, A finite element moving boundary computation with an adaptive mesh, J. Inst. Maths Applics 22 (1978) 467–477.
[15] R.M. Furzeland, A comparative study of numerical methods for moving boundary problems, J. Inst. Maths Applics 26 (1980) 411–429.
[16] R.S. Gupta, N.C. Banik, Diffusion of oxygen in a sphere with simultaneous absorption, Appl. Math. Model. 14 (1990) 114–121.
[17] J. Crank, Free and Moving Boundary Problems, Clarendon Press, Oxford, 1984.
[18] M. Zerroukat, R. Chatwin, An explicit unconditionally stable variable time step method for 1D Stefan problems, Int. J. Numer. Methods Eng. 35 (1992) 1503–1520.
[19] S.G. Ahmed, A numerical method for oxygen diffusion and absorption in a sick cell, Appl. Math. Comput. 173 (2006) 668–682.
[20] A. Boureghda, Numerical solution of the oxygen diffusion in absorbing tissue with a moving boundary, Commun. Numer. Methods Eng. 22 (2006) 933–942.
[21] A. Boureghda, Numerical solution of the oxygen diffusion problem in cylindrically shaped sections of tissue, Int. J. Numer. Methods Fluids 56 (2008) 1945–1960.
[22] S.L. Mitchell, An accurate application of the integral method applied to the diffusion of oxygen in absorbing tissue, Appl. Math. Model. 38 (2014) 4396–4408.
[23] S.L. Mitchell, M. Vynnycky, An accurate finite-difference method for ablation-type Stefan problems, J. Comput. Appl. Maths 236 (2012) 4181–4192.
[24] S.L. Mitchell, M. Vynnycky, I.G. Gusev, S.S. Sazhin, An accurate numerical solution for the transient heating of an evaporating droplet, Appl. Math. Comput. 217 (2011) 9219–9233.
[25] M. Vynnycky, S.L. Mitchell, On the accuracy of a finite-difference method for parabolic PDEs with discontinuous boundary conditions, Numer. Heat Transfer B 64 (2013) 275–292.
[26] M. Vynnycky, A mathematical model for air-gap formation in vertical continuous casting: the effect of superheat, Trans. Ind. Inst. Metals 62 (2009) 495–498.
[27] M. Vynnycky, An asymptotic model for the formation and evolution of air gaps in vertical continuous casting, Proc. R. Soc. A: Math. Phys. Eng. Sci. 465 (2009) 1617–1644.
[28] M. Vynnycky, Air gaps in vertical continuous casting in round moulds, J. Eng. Maths 68 (2010) 129–152.
[29] M. Vynnycky, On the role of radiative heat transfer in air gaps in vertical continuous casting, Appl. Math. Model. 37 (2013) 2178–2188.
[30] M. Vynnycky, On the onset of air-gap formation in vertical continuous casting with superheat, Int. J. Mech. Sci. 73 (2013) 69–76.
[31] S.W. McCue, M. Hsieh, T.J. Moroney, M.I. Nelson, Asymptotic and numerical results for a model of solvent-dependent drug diffusion through polymeric spheres, SIAM J. Appl. Math. 71 (2011) 2287–2311.
[32] S.L. Mitchell, M. Vynnycky, Finite-difference methods with increased accuracy and correct initialization for one-dimensional Stefan problems, Appl. Math. Comput. 215 (2009) 1609–1621.
[33] J. Åberg, M. Vynnycky, H. Fredriksson, Heat-flux measurements of industrial on-site continuous copper casting and their use as boundary conditions for numerical simulations, Trans. Ind. Inst. Metals 62 (2009) 443–446.
[34] M. Vynnycky, A mathematical model for air-gap formation in vertical continuous casting: the effect of superheat, Trans. Ind. Inst. Metals 62 (2009) 495–498.
[35] S.L. Mitchell, M. Vynnycky, On the numerical solution of two-phase Stefan problems with heat-flux boundary conditions, J. Comput. Appl. Math. 264 (2014) 49–64.
[36] J.C. Strikwerda, Finite Difference Schemes and Partial Differential Equations, second ed., Society for Industrial Mathematics, 2004.
[37] M. Vynnycky, S.L. Mitchell, On the numerical solution of a Stefan problem with finite extinction time, J. Comput. Appl. Math. 276 (2015) 98–109.